Electronic Supplementary Material (ESI) for Journal of Materials Chemistry A.

Electronic Supplementary Information

Molecular Engineering of Acceptors to Control Aggregation for Optimized Nonfullerene Solar Cells

Linqiang Yang, Zhenghao Hu, Zhuohan Zhang, Jinru Cao, Hongtao Wang, Jiangsheng Yu, Fujun Zhang, Weihua Tang**

Table of Contents

1. Materials and Synthesis

All commercially available chemicals and solvents were used directly without further purification unless otherwise stated. Tetrahydrofuran (THF) and toluene were distilled before a drying progress of sodium, and 1,2-dichloroethane was dried with calcium hydride. 4-(2-butyloctyl)-2-(tributylstannyl)-4H-dithieno[3,2-*b*:2',3'-*d*]pyrrole (compound **1**) and IPT-CHO were synthesized according to the literature.[1,2]

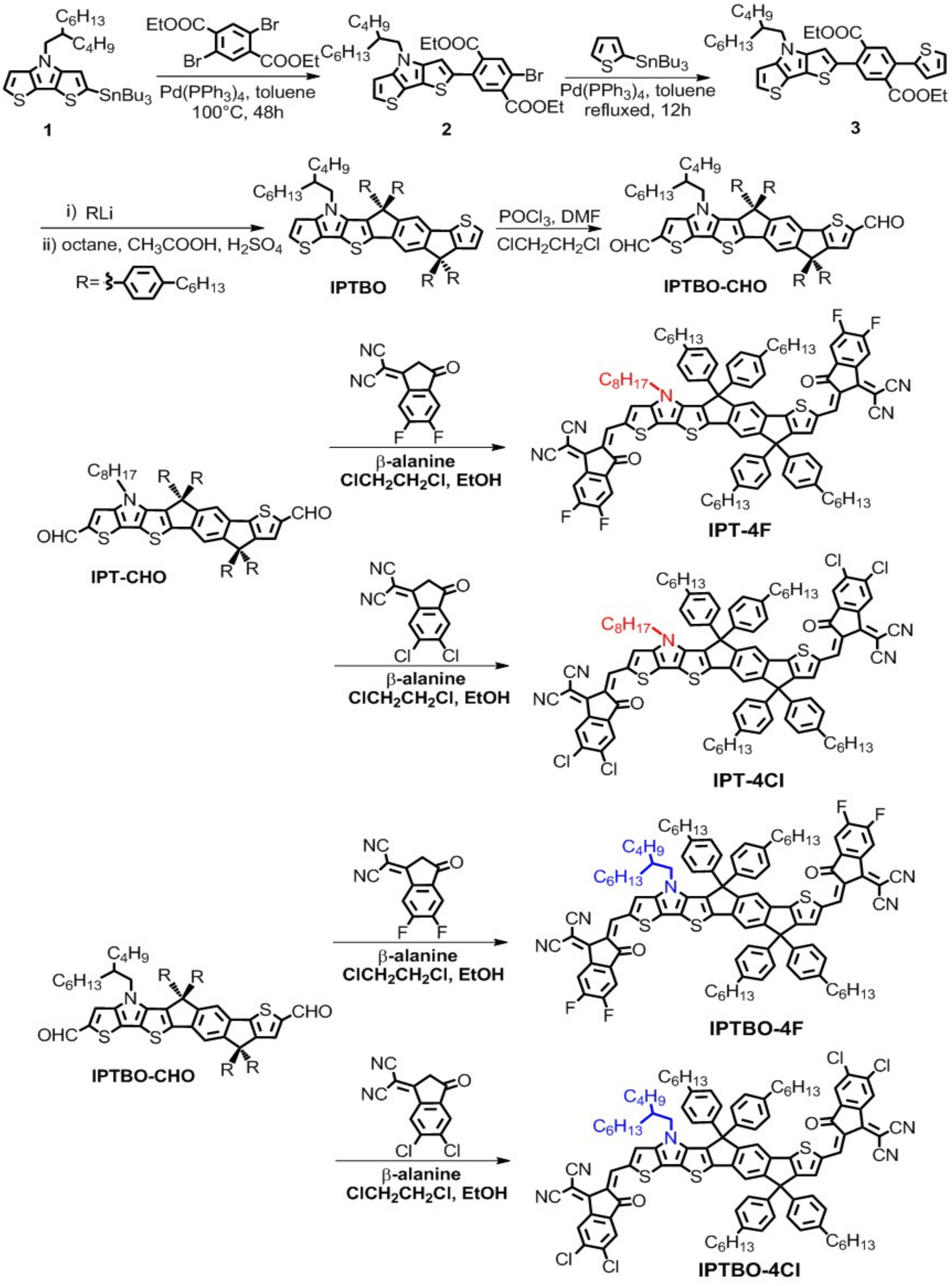

Scheme S1. Synthetic routes of IPT-4F, IPTBO-4F, IPT-4Cl, and IPTBO-4Cl.

Synthesis of diethyl 2-bromo-5-(4-(2-butyloctyl)-4H-dithieno[3,2-*b*:2',3'-*d*]pyrrol-2-yl)terephthalate (compound 2): diethyl 2,5-dibromoterephthalate (5.0 g, 13.2 mmol), compound 1 (4.2 g, 6.6 mmol), $Pd(PPh_3)_4$ (152.5 mg, 131.9 µmol) were added in anhydrous toluene (100 mL). The mixture reacted at 100°C for 48 h under nitrogen and then cooled to room temperature. The solvent in the mixture was evaporated under vacuum. The residue was purified by silica gel column chromatography (petroleum ether/ethyl acetate=15:1 v/v) to obtain an orange viscous liquid (2.4 g, 56%). ^{1}H NMR (500 MHz, $CDCl_3$, δ): 7.96 (s, 1H), 7.95 (s, 1H), 7.16 (d, 1H), 7.02 (s, 1H), 6.98 (d, 1H), 4.44 (m, 2H), 4.24 (m, 2H), 4.04 (m, 2H), 2.04 – 1.98 (m, 1H), 1.42 (m, 3H), 1.28 (m, 16H), 1.16 (m, 3H), 0.86 (m, 6H). ^{13}C NMR (125 MHz, $CDCl_3$, δ): 167.05, 165.40, 145.34, 145.05, 136.42, 135.33, 134.81, 134.49, 134.16, 133.38, 123.85, 120.12, 115.96, 114.76, 111.37, 111.15, 62.17, 61.98, 51.89, 39.17, 31.86, 31.70, 31.39, 29.67, 28.77, 26.55, 23.08, 22.70, 14.29, 14.18, 14.12, 14.04.

Synthesis of diethyl 2-(4-(2-butyloctyl)-4H-dithieno[3,2-b:2',3'-d]pyrrol-2-yl)-5-(thiophen-2-yl)terephthalate (compound 3): Compound 2 (700.0 mg, 1.1 mmol), tributyl(thiophen-2-yl)stannane (525.1 mg, 1.4 mmol), $Pd(PPh_3)_4$ (50.0 mg, 43.3 µmol) were added in anhydrous toluene (12 mL). The mixture reacted for 12 h under nitrogen. The solvent in the mixture was evaporated under vacuum. The residue was purified by silica gel column chromatography (petroleum ether/dichloromethane=3:2 v/v) to obtain an orange viscous liquid (600 mg, 85%). ^{1}H NMR (500 MHz, $CDCl_3$, δ): 7.90 (s, 1H), 7.79 (s, 1H), 7.39 (d, 1H), 7.16 (d, 1H), 7.11 (d, 1H), 7.10 – 7.07 (m, 1H), 7.05 (s, 1H), 6.99 (d, 1H), 4.24 (m, 4H), 4.05 (m, 2H), 2.04 – 1.98 (m, 1H), 1.35 – 1.21 (m, 16H), 1.16 (m, 6H), 0.86 (m, 6H). ^{13}C NMR (125 MHz, $CDCl_3$, δ): 168.31, 167.95, 145.34, 145.18, 140.77, 137.33, 134.36, 134.16, 134.13, 133.10, 131.85, 131.82, 127.51, 127.08, 126.58, 123.76, 115.97, 114.85, 111.24, 111.20, 61.87, 61.80, 51.98, 39.25, 31.94, 31.77, 31.46, 29.75, 28.85, 26.62, 23.16, 22.77, 14.25, 14.20, 14.13, 13.98.

Synthesis of IPTBO: A solution of 4-hexyl-1-bromobenzene (1.8 g, 7.5 mmol) in anhydrous THF (40 mL) was placed at -78°C for 10 min, then *n*-BuLi (2.8 mL, 7.0 mmol, 2.5 M in hexane) was added to the solution slowly. After the mixture was stirred for 2 h at -78°C under nitrogen, compound 3 (650.0 mg, 1.0 mmol) in THF (5 mL) was then added to the solution in a minute. The reaction mixture was warmed to room temperature and stirred for 2 h. The solvent of the mixture was evaporated under vacuum. The light yellow residue was dissolved in octane (80 mL) and acetic acid (40 mL), then 0.1 mL concentrated H_2SO_4 was added dropwise. The solution was stirred at room temperature for 1 h before quenched by water. The organic layer was extracted with petroleum ether (2×60 mL) and washed with water for two times. The combined organic phase was dried over anhydrous $MgSO_4$. The solvent in the mixture was evaporated under vacuum, and the residue was purified by silica gel column chromatography (petroleum ether/dichloromethane=9:1 v/v) to obtain a viscous yellow liquid (1.0 g, 85%). ^{1}H NMR (500 MHz, CD_2Cl_2, δ): 7.44 (s, 1H), 7.40 (s, 1H), 7.35 (m, 4H), 7.27 (d, 1H), 7.16 (d, 4H), 7.09 (m, 9H), 6.99 (d, 1H), 6.95 (d, 1H), 3.65 (m, 2H), 2.57 (m, 8H), 1.67 (m, 1H), 1.58 (m, 8H), 1.39 – 0.65 (m, 58H). ^{13}C NMR (125 MHz, CD_2Cl_2, δ): 157.16, 156.05, 153.84, 144.97, 142.46, 142.41, 142.06, 141.62, 141.15, 140.67, 140.63, 138.97, 138.92, 135.99, 135.22, 129.35, 128.84, 128.76, 128.15, 127.84, 123.38, 122.96, 118.16, 116.62, 116.36, 116.17, 112.85, 63.15, 63.08, 53.27, 37.88, 36.34, 35.90, 32.16, 32.01, 31.92, 31.90, 31.14, 30.90, 29.95, 29.56, 29.55, 29.44, 29.34, 27.05, 23.32, 23.03, 14.30, 14.18.

Synthesis of IPTBO-CHO: A mixed solution of compound IPTBO (900.0 mg, 768.7 μmol) in anhydrous DMF (4 mL) and anhydrous 1,2-dichloroethane (12 mL) was placed at 0°C for 10 min, then phosphorus oxychloride ($POCl_3$, 0.6 mL) was slowly added to the solution under nitrogen. After being stirred at 0°C for several minutes, the mixture was warmed to 70°C for 3 h. The reaction mixture was poured into a solution of Na_2CO_3 (21.2 g, 0.2 mol) in water (150 mL). The mixture was vigorously stirred at room temperature for 6 h. The organics were extracted with a mixed solvent of ethyl acetate and petroleum ether (1:9, v/v). The combined organic layer was washed with water and dried with anhydrous Mg_2SO_4. The solvent was evaporated under vacuum, and the residue was purified by silica gel column chromatography (petroleum ether/dichloromethane=3:2 v/v) to obtain an orange solid (820 mg, 87%). ^{1}H NMR (500 MHz, CD_2Cl_2, δ): 9.83 (s, 1H), 9.79 (s, 1H), 7.64 (s, 1H), 7.59 (s, 1H), 7.57 (s, 1H), 7.50 (s, 1H), 7.33 (m, 4H), 7.13 (m, 12H), 3.68 (m, 2H), 2.57 (m, 8H), 1.70 – 1.63 (m, 1H), 1.60 – 1.55 (m, 8H), 1.37 –0.65 (m, 58H). ^{13}C NMR (125 MHz, CD_2Cl_2, δ): 183.05, 158.11, 156.65, 155.31, 151.01, 146.24, 145.63, 145.10, 144.46, 142.95, 142.61, 141.28, 140.89, 140.61, 138.03, 137.98, 137.69, 134.73, 132.33, 129.24, 129.07, 129.00, 128.04, 124.53, 121.34, 119.15, 118.11, 117.05, 63.34, 63.32, 38.14, 35.87, 32.12, 31.87, 31.84, 31.16, 30.94, 29.92, 29.53, 29.50, 29.34, 27.05, 23.32, 23.01, 22.99, 14.27, 14.15. MALDI-TOF MS (*m*/*z*): $[M+H]^+$ calcd. for $C_{82}H_{99}NO_2S_3$, 1225.6838; found, 1225.6832.

Synthesis of IPT-4F: Compound IPT-CHO (120.0 mg, 102.5 μmol), 2-(5,6-difluoro-3-oxo-2,3-dihydro-1H-inden-1-ylidene) malononitrile (118.0 mg, 512.5 μmol) and β-alanine (1.8 mg, 20.5 μmol) were dissolved in a mixed solvent of 1,2-dichloroethane (8 mL) and EtOH (3 mL). The mixture was placed at 60°C for several hours and the reaction process was monitored by TLC. The solvent in the mixture was evaporated under vacuum. The residue was purified by silica gel column chromatography (petroleum ether/dichloromethane=3:2 v/v) to obtain a dark-blue solid (130 mg, 80%). ^{1}H NMR (500 MHz, $CDCl_3$, δ): 8.85 (d, 2H), 8.50 (m, 2H), 7.71 – 7.56 (m, 5H), 7.51 (s, 1H), 7.31 (m, 4H), 7.16 – 7.10 (m, 12H), 3.81 – 3.75 (m, 2H), 2.59 (m, 8H), 1.64 – 1.58 (m, 8H), 1.37 – 1.26 (m, 28H), 1.19 (m, 4H), 1.06 (m, 4H), 0.90 – 0.86 (m, 15H). ^{13}C NMR (125 MHz, $CDCl_3$, δ): 186.27, 186.08, 161.07, 158.83, 158.63, 158.47, 157.99, 156.69, 155.73, 153.34, 153.23, 150.75, 147.52, 146.87, 142.94, 142.58, 140.84, 140.72, 140.47, 140.30, 138.90, 138.83, 138.60, 137.14, 136.75, 136.68, 136.58, 135.55, 134.67, 134.57, 128.97, 128.95, 128.66, 127.91, 121.02, 120.43, 119.68, 118.99, 117.73, 115.29, 115.19, 115.08, 115.00, 114.83, 114.51, 114.43, 112.83, 112.68, 112.57, 112.43, 69.55, 67.45, 63.13, 62.81, 48.76, 35.76, 35.74, 32.07, 31.91, 31.89, 31.51, 31.46, 30.63, 29.53, 29.45, 29.36, 29.30, 26.99, 22.87, 22.79, 14.32, 14.30, 14.29. MALDI-TOF MS (*m*/*z*): $[M+H]^+$ calcd. for $C_{102}H_{95}F_4N_5O_2S_3$, 1593.6584; found, 1593.6585.

Synthesis of IPT-4Cl: Compound IPT-CHO (120.0 mg, 102.5 μmol), 2-(5,6-dichloro-3-oxo-2,3-dihydro-1H-inden-1-ylidene) malononitrile (134.8 mg, 512.5 μmol) and β-alanine (1.8 mg, 20.5 μmol) were dissolved in a mixed solvent of 1,2-dichloroethane (8 mL) and EtOH (3 mL). The mixture was placed at 60°C for several hours and the reaction process was monitored by TLC. The solvent in the mixture was evaporated under vacuum. The residue was purified by silica gel column chromatography (petroleum ether/dichloromethane=3:2 v/v) to obtain a dark-blue solid (135 mg, 79%). ^{1}H NMR (500 MHz, $CDCl_3$, δ): 8.87 (s, 1H), 8.81 (s, 1H), 8.74 (s, 1H), 8.64 (s, 1H), 7.89 (s, 1H), 7.84 (s, 1H), 7.69 (d, 2H), 7.51 (m, 2H), 7.31 (d, 4H), 7.14 (m, 12H), 3.81 – 3.75 (m, 2H), 2.59 (m, 8H), 1.63 – 1.57 (m, 8H), 1.36 – 1.26 (m, 28H), 1.23 – 0.98 (m, 8H), 0.87 (m, 15H). ^{13}C NMR (125 MHz, $CDCl_3$, δ): 186.32, 186.08, 161.53, 158.70, 158.61, 158.35, 158.16, 156.82, 151.17, 147.83, 147.06, 142.99, 142.60, 141.16, 140.76, 140.43, 139.84, 139.53, 139.36, 139.14, 139.00, 138.92, 138.86, 138.82, 137.10, 136.94, 136.21, 135.63, 128.99, 128.97, 128.67, 127.92, 127.17, 126.79, 126.34, 125.29, 124.96, 121.03, 120.62, 119.58, 119.10, 117.82, 115.28, 115.10, 114.51, 69.61, 67.47, 63.14, 62.85, 48.79, 35.77, 35.75, 32.08, 31.91, 31.89, 31.51, 31.46, 30.63, 29.54, 29.44, 29.36, 29.31, 27.00, 22.87, 22.79, 14.32, 14.30, 14.29. MALDI-TOF MS (*m*/*z*): $[M+H]^+$ calcd. for $C_{102}H_{95}Cl_4N_5O_2S_3$, 1657.5402; found, 1657.5397.

Synthesis of IPTBO-4F: Compound IPTBO-CHO (120.0 mg, 97.8 μmol), 2-(5,6-difluoro-3-oxo-2,3-dihydro-1H-inden-1-ylidene) malononitrile (112.6 mg, 489.1 μmol) and β-alanine (1.7 mg, 19.6 μmol) were dissolved in a mixed solvent of 1,2-dichloroethane (8 mL) and EtOH (3 mL). The mixture was placed at 60°C for several hours and the reaction process was monitored by TLC. The solvent in the mixture was evaporated under vacuum. The residue was purified by silica gel column chromatography (petroleum ether/dichloromethane=3:2 v/v) to obtain a dark-blue solid (130 mg, 80%). ^{1}H NMR (500 MHz, $CDCl_3$, δ): 8.86 (s, 1H), 8.84 (s, 1H), 8.51 (m, 2H), 7.72 – 7.60 (m, 5H), 7.50 (s, 1H), 7.32 – 7.27 (m, 4H), 7.12 (m, 12H), 3.68 (m, 2H), 2.59 (m, 8H), 1.68 – 1.57 (m, 9H), 1.38 – 0.65 (m, 58H). ^{13}C NMR (125 MHz, $CDCl_3$, δ): 186.27, 186.04, 161.09, 158.97, 158.89, 158.49, 157.98, 156.65, 155.74, 155.63, 155.46, 153.38, 150.99, 148.60, 146.84, 142.98, 142.58, 140.83, 140.68, 140.48, 140.29, 138.83, 138.71, 138.67, 137.20, 137.16, 136.76, 136.71, 136.69, 136.44, 135.57, 134.67, 129.02, 128.95, 127.91, 121.03, 120.46, 119.84, 118.97, 117.64, 115.30, 115.12, 115.09, 115.02, 114.84, 114.52, 114.43, 112.84, 112.60, 112.46, 69.56, 67.58, 63.13, 63.07, 53.40, 37.84, 35.76, 35.75, 31.91, 31.88, 31.57, 31.51, 31.01, 30.75, 29.77, 29.34, 29.30, 29.06, 26.83, 23.14, 22.79, 14.29, 14.15. MALDI-TOF MS (*m/z*): $[M+H]^+$ calcd. for $C_{106}H_{103}F_4N_5O_2S_3$, 1649.7210; found, 1649.7215.

Synthesis of IPTBO-4Cl: Compound IPTBO-CHO (120.0 mg, 97.8 μmol), 2-(5,6-dichloro-3-oxo-2,3-dihydro-1H-inden-1-ylidene) malononitrile (128.7 mg, 489.1 μmol) and β-alanine (1.7 mg, 19.6 μmol) were dissolved in a mixed solvent of 1,2-dichloroethane (8 mL) and EtOH (3 mL). The mixture was placed at 60°C for several hours and the reaction process was monitored by TLC. The solvent in the mixture was evaporated under vacuum. The residue was purified by silica gel column chromatography (petroleum ether/dichloromethane=3:2 v/v) to obtain a dark-blue solid (136 mg, 81%). ^{1}H NMR (500 MHz, $CDCl_3$, δ): 8.87 (s, 1H), 8.80 (s, 1H), 8.74 (s, 1H), 8.65 (s, 1H), 7.89 (s, 1H), 7.85 (s, 1H), 7.72 – 7.48 (m, 4H), 7.31 (m, 4H), 7.13 (m, 12H), 3.68 (m, 2H), 2.59 (m, 8H), 1.60 (m, 9H), 1.37 – 0.65 (m, 58). ^{13}C NMR (125 MHz, $CDCl_3$, δ): 186.32, 186.05, 161.57, 159.03, 158.62, 158.34, 158.12, 156.74, 151.44, 148.89, 147.00, 143.01, 142.59, 141.13, 140.68, 140.45, 140.42, 139.82, 139.51, 139.35, 139.14, 138.97, 138.90, 138.84, 138.80, 137.12, 137.08, 136.77, 136.19, 135.63, 129.03, 128.95, 127.90, 127.15, 126.78, 125.28, 124.95, 120.97, 120.64, 119.63, 119.07, 117.72, 115.22, 115.10, 114.50, 69.57, 67.56, 63.10, 63.06, 53.41, 37.81, 35.75, 31.91, 31.88, 31.59, 31.52, 30.98, 30.73, 29.78, 29.34, 29.30, 29.03, 26.81, 23.14, 22.80, 14.30, 14.17. MALDI-TOF MS (*m/z*): $[M+H]^+$ calcd. for $C_{106}H_{103}Cl_4N_5O_2S_3$, 1713.6028; found, 1713.6028.

2. NMR and Mass Spectra

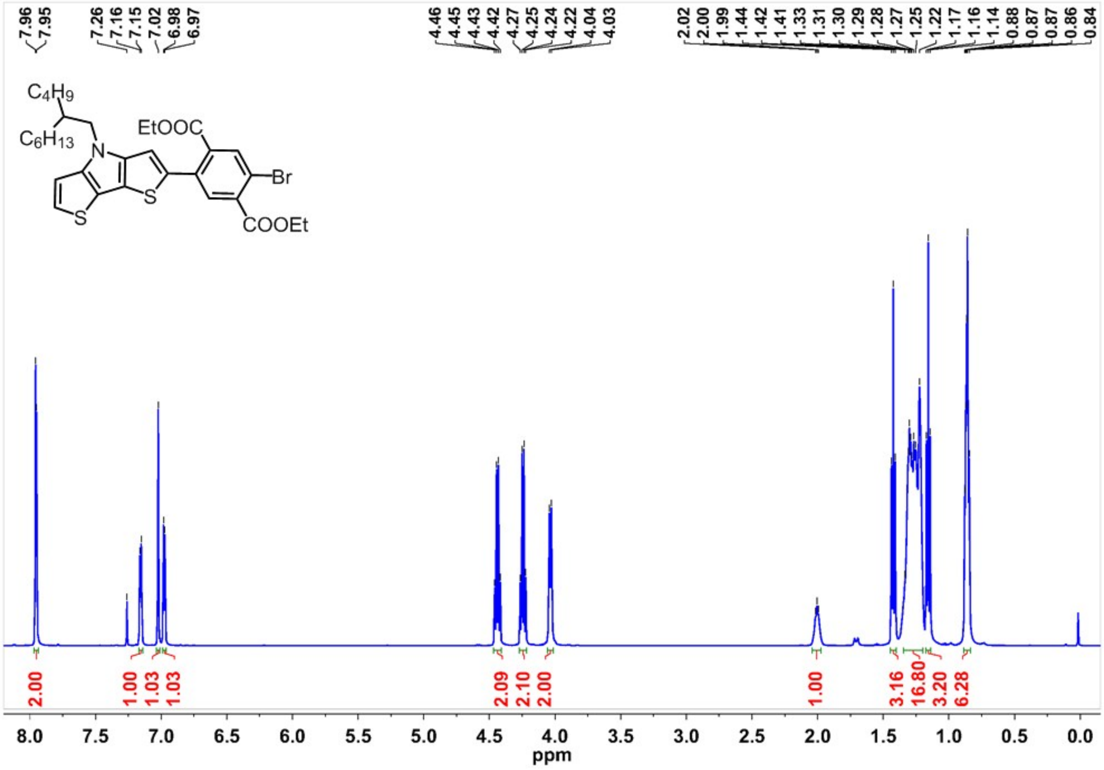

Figure S1. ^{1}H NMR spectrum of Compound **2.**

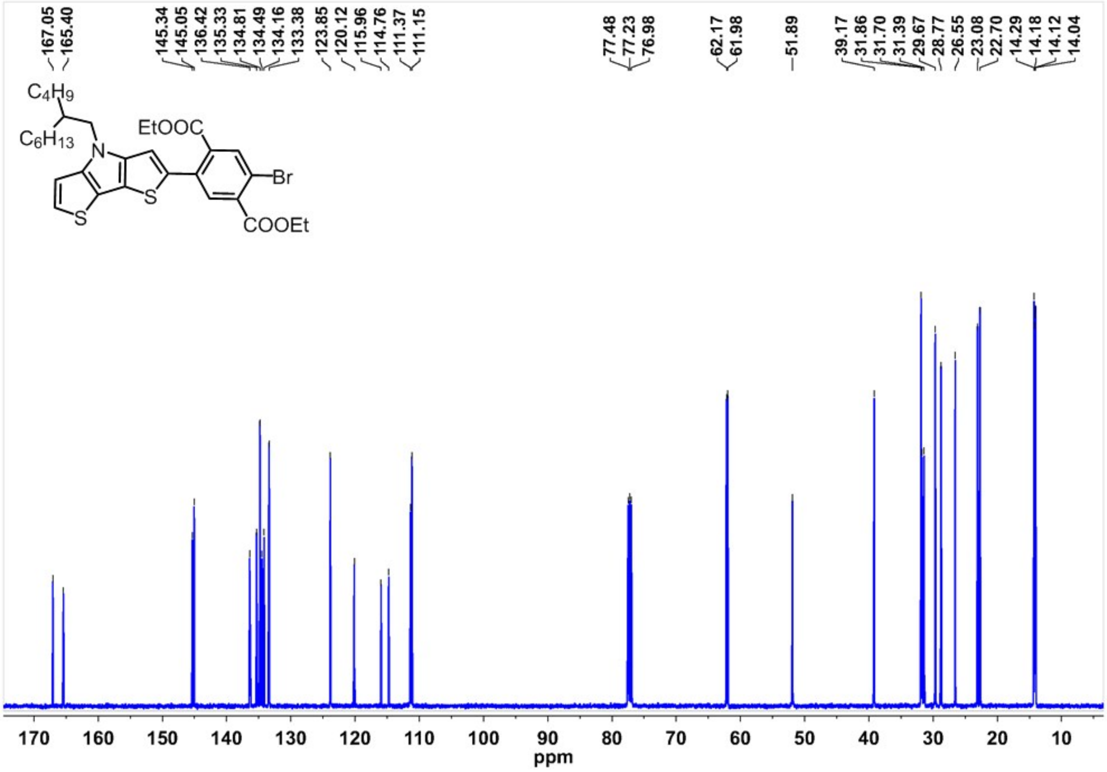

Figure S2. ^{13}C NMR spectrum of Compound **2**.

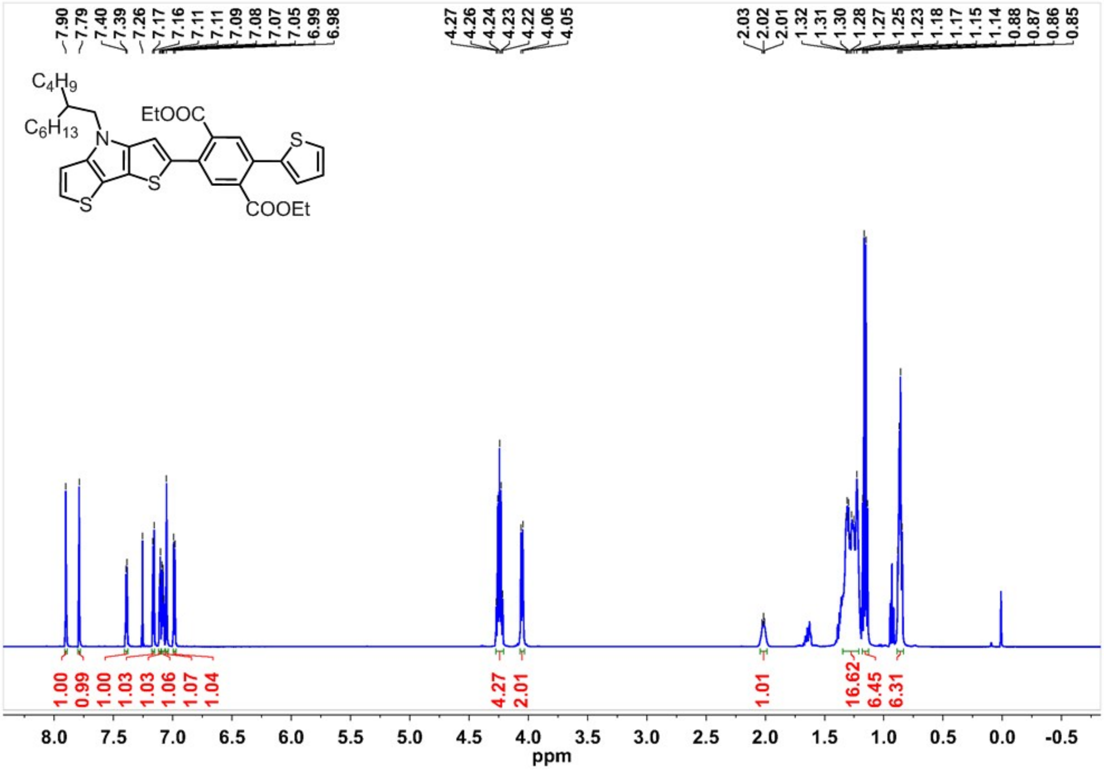

Figure S3. ^{1}H NMR spectrum of Compound **3**.

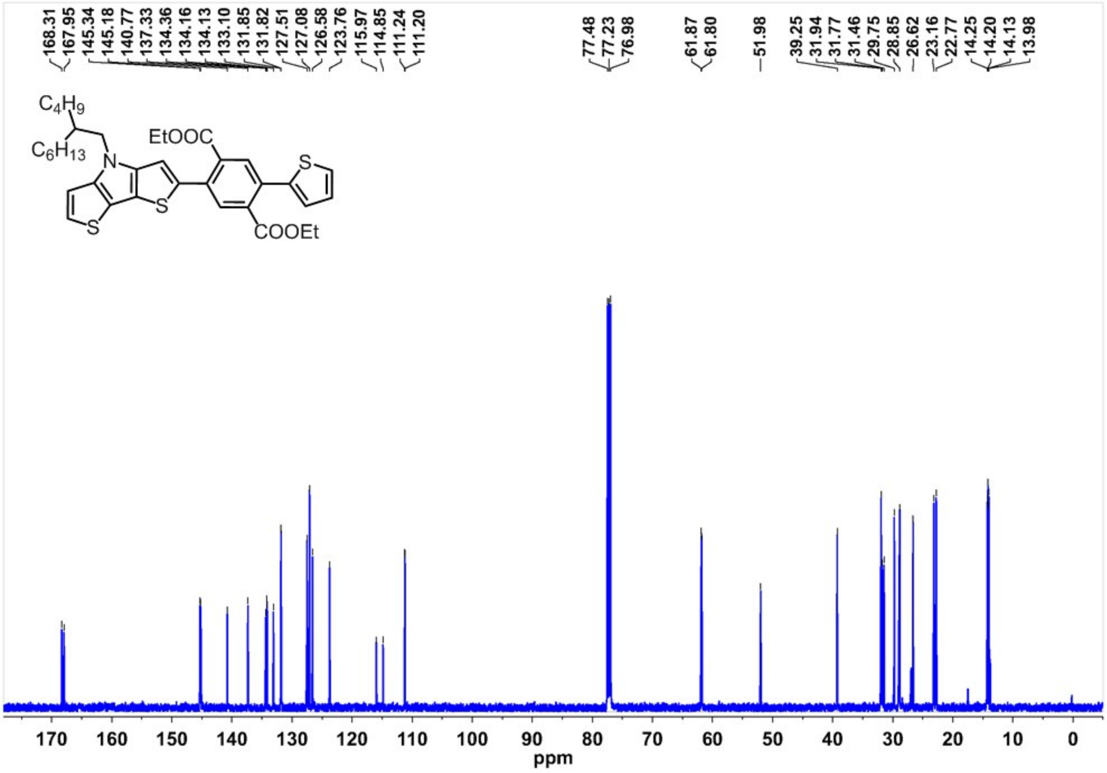

Figure S4. ^{13}C NMR spectrum of Compound 3.

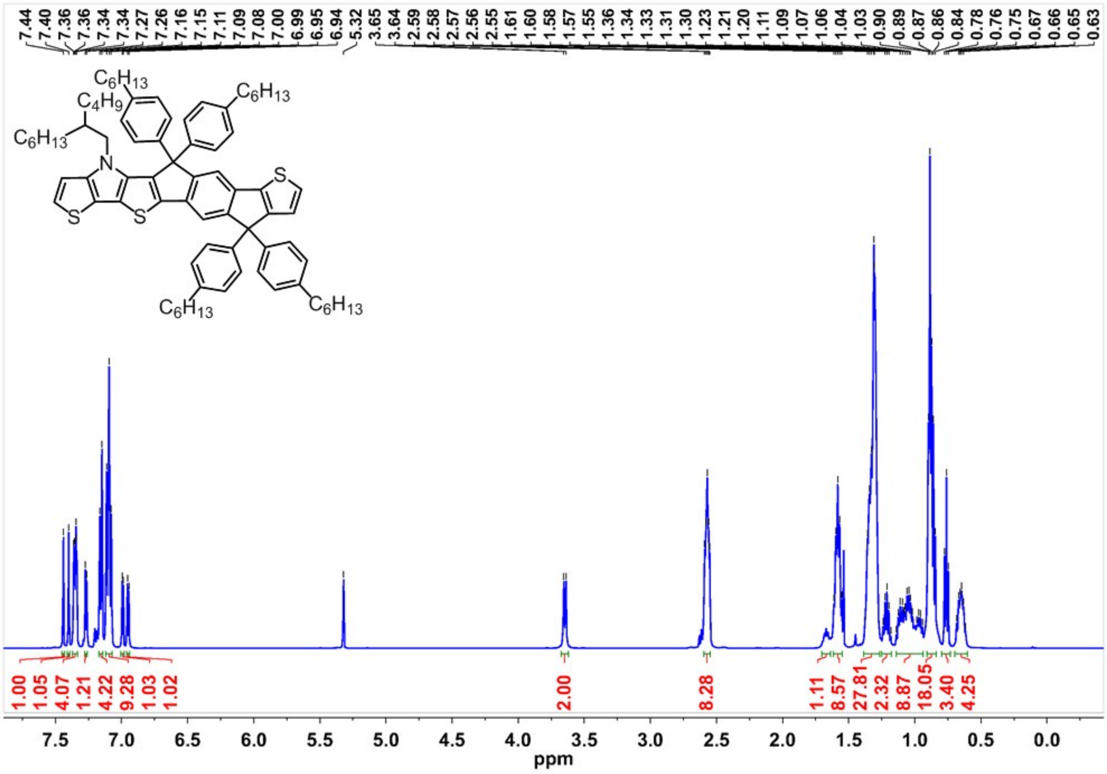

Figure S5. ${}^{1}H$ NMR spectrum of IPTBO.

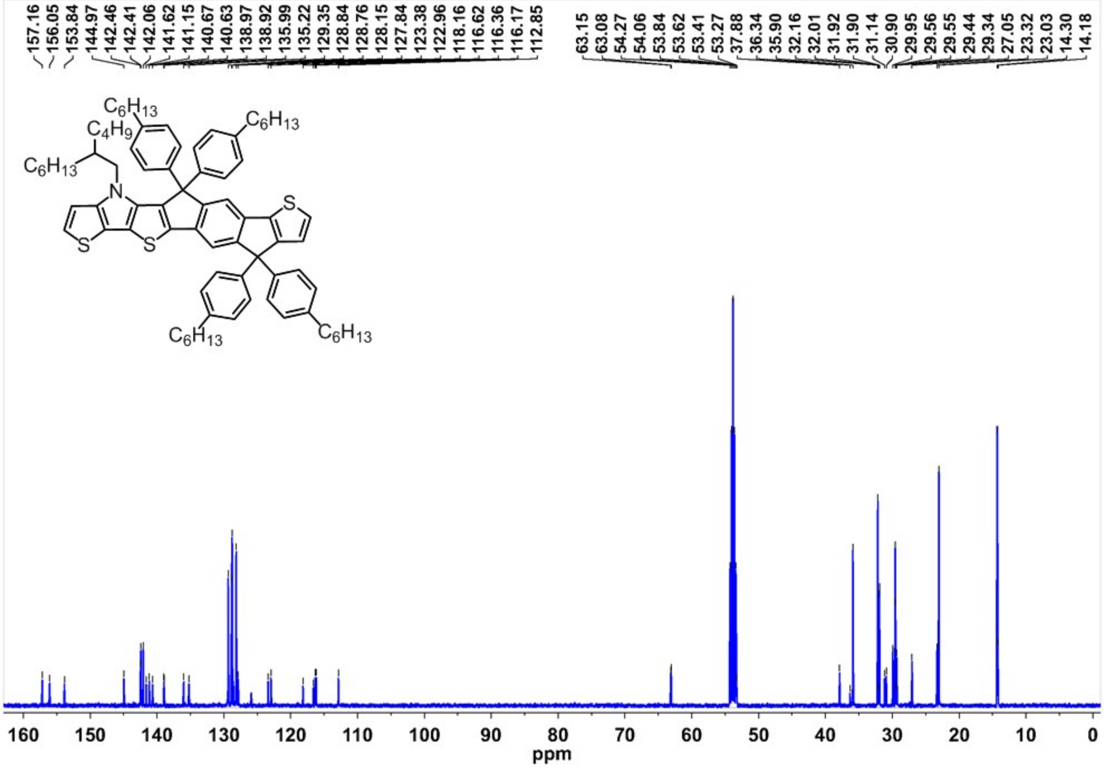

Figure S6. ${}^{13}C$ NMR spectrum of IPTBO.

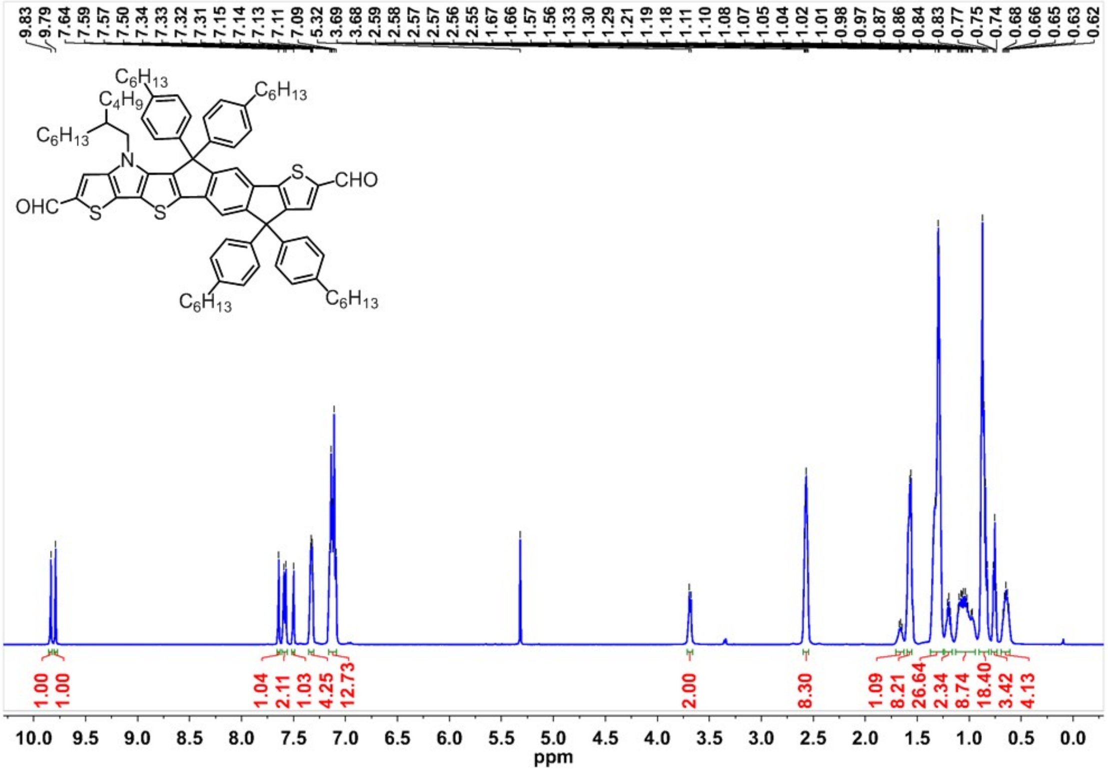

Figure S7. ^{1}H NMR spectrum of IPTBO-CHO.

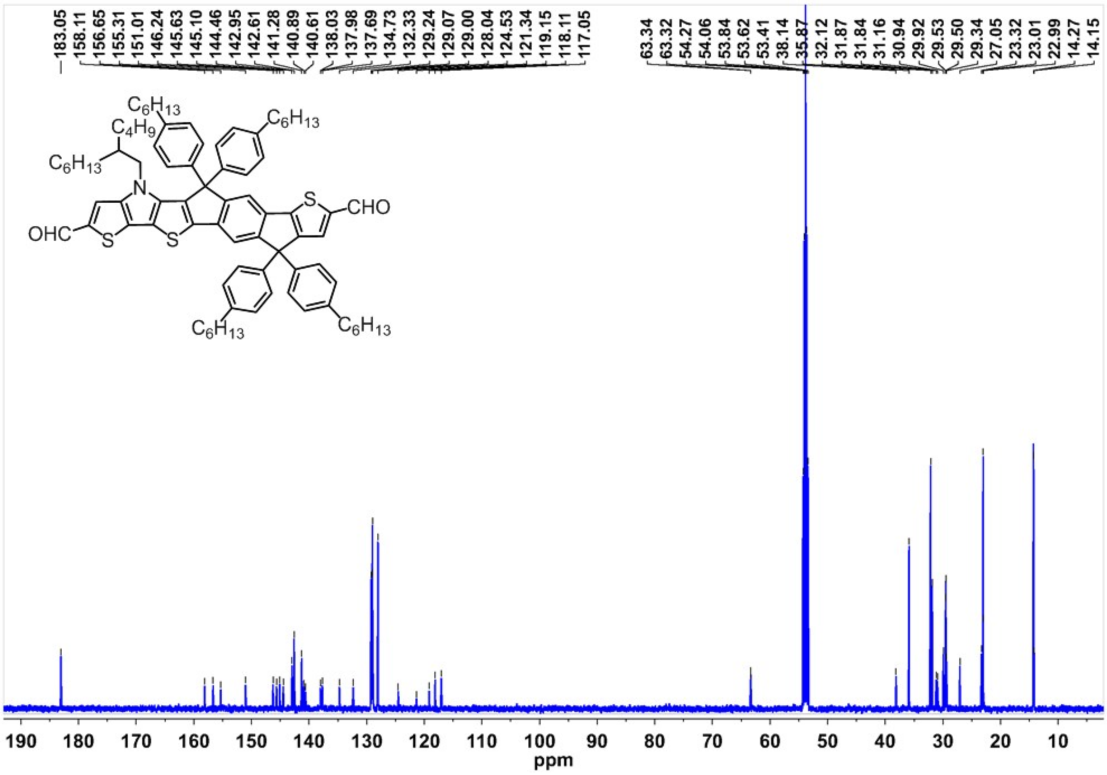

Figure S8. ^{13}C NMR spectrum of IPTBO-CHO.

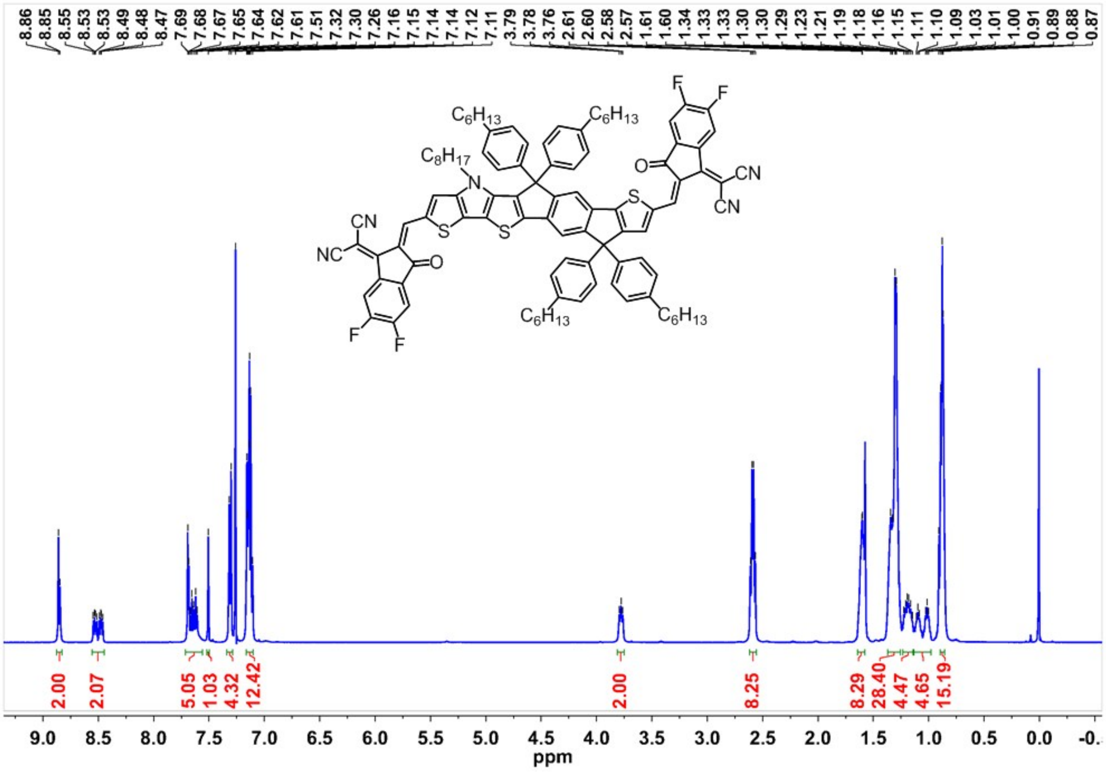

Figure S9. ^{1}H NMR spectrum of IPT-4F.

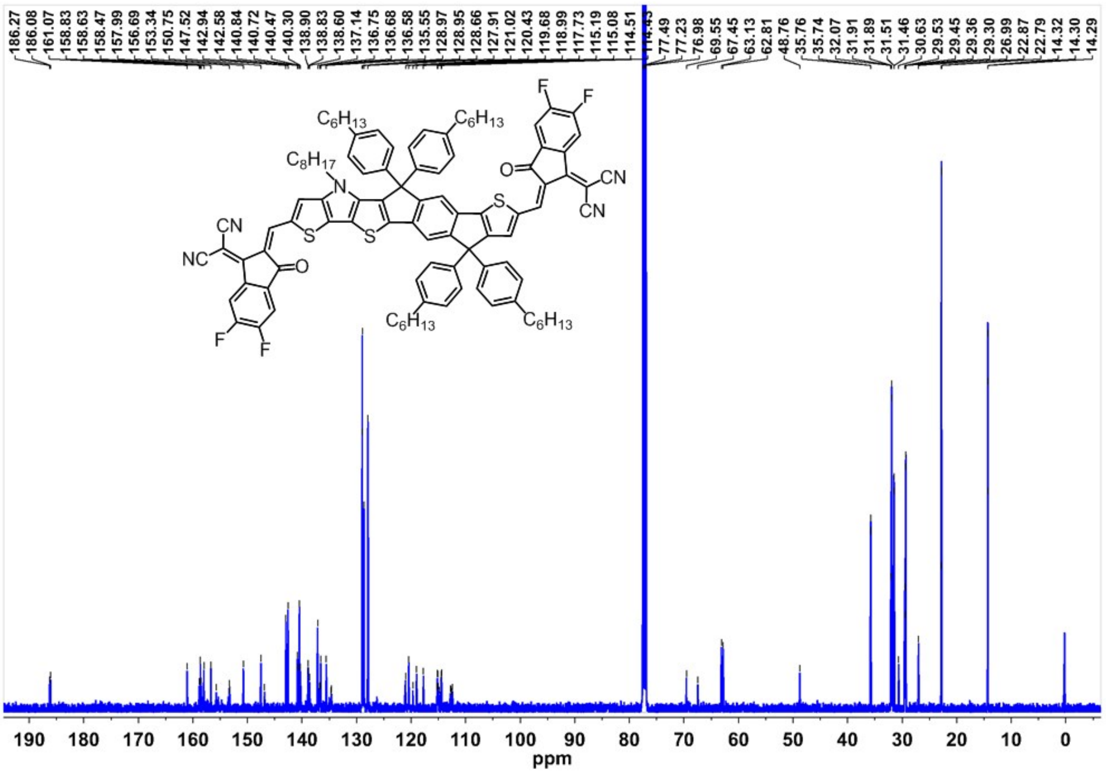

Figure S10. ^{13}C NMR spectrum of IPT-4F.

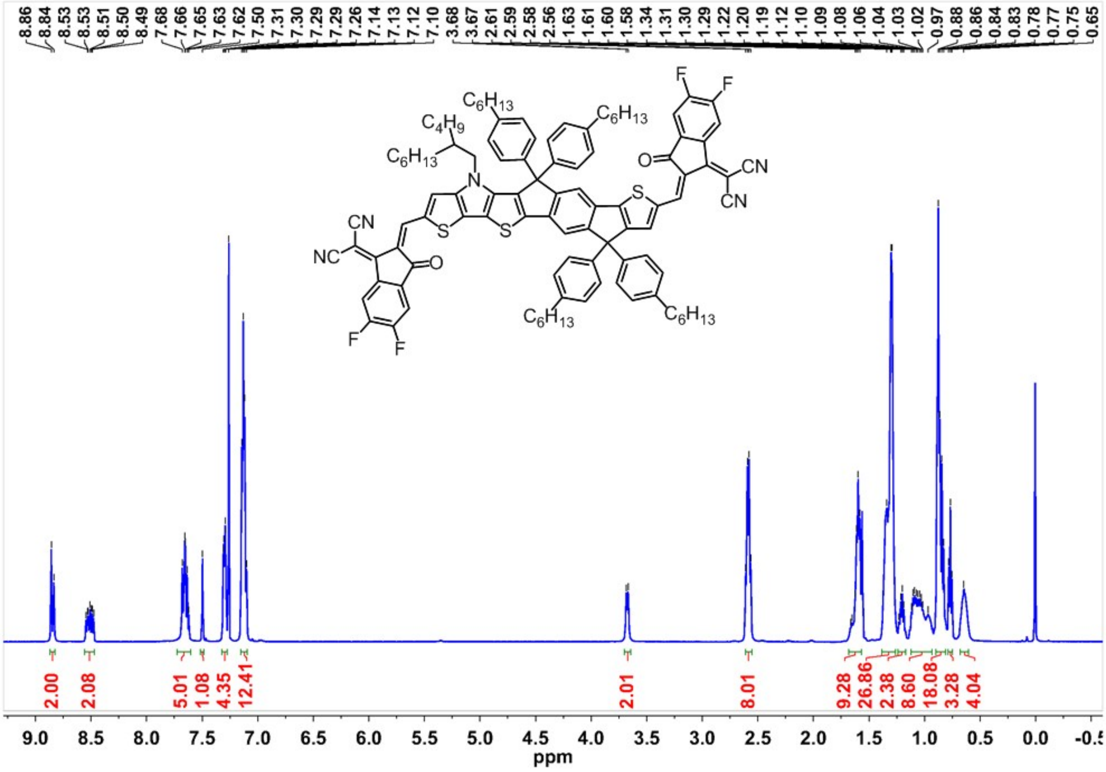

Figure S11. ^{1}H NMR spectrum of IPTBO-4F.

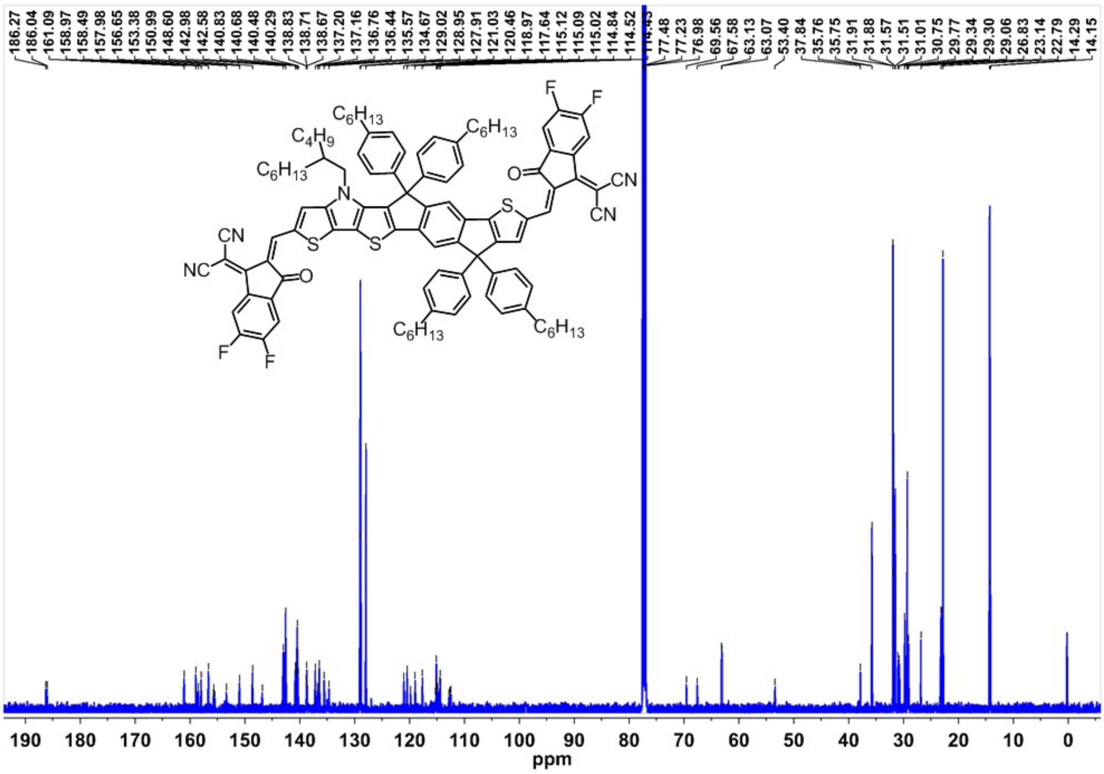

Figure S12. ^{13}C NMR spectrum of IPTBO-4F.

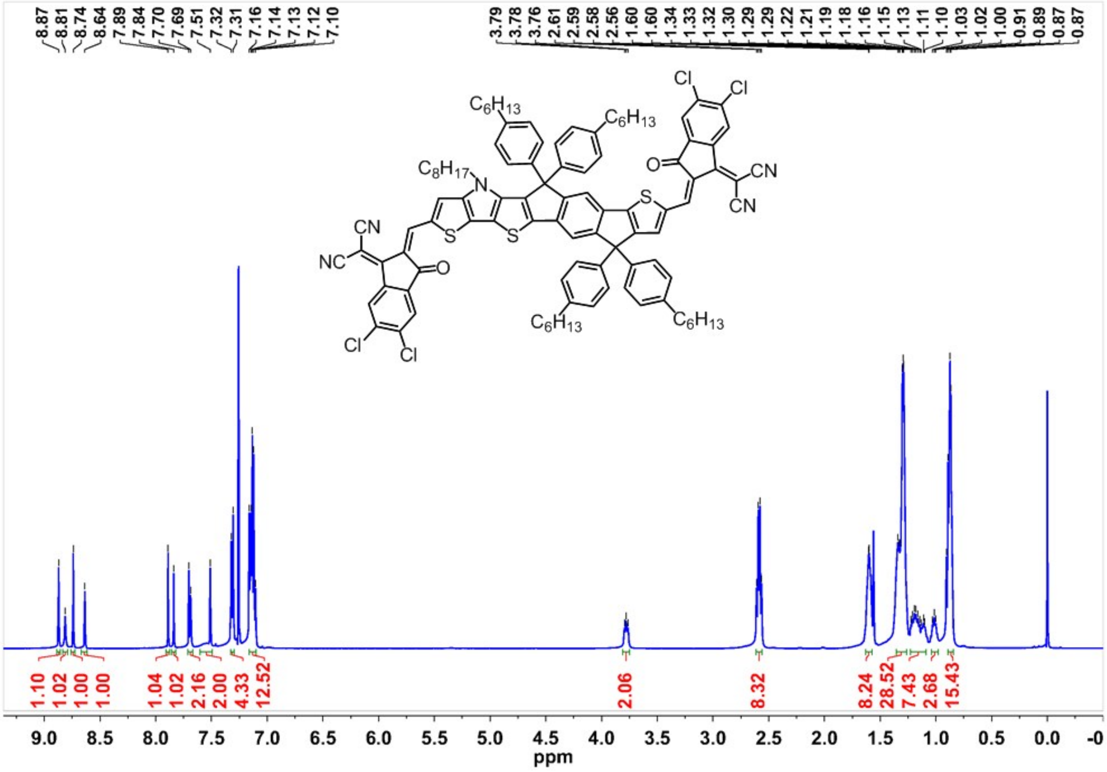

Figure S13. ^{1}H NMR spectrum of IPT-4Cl.

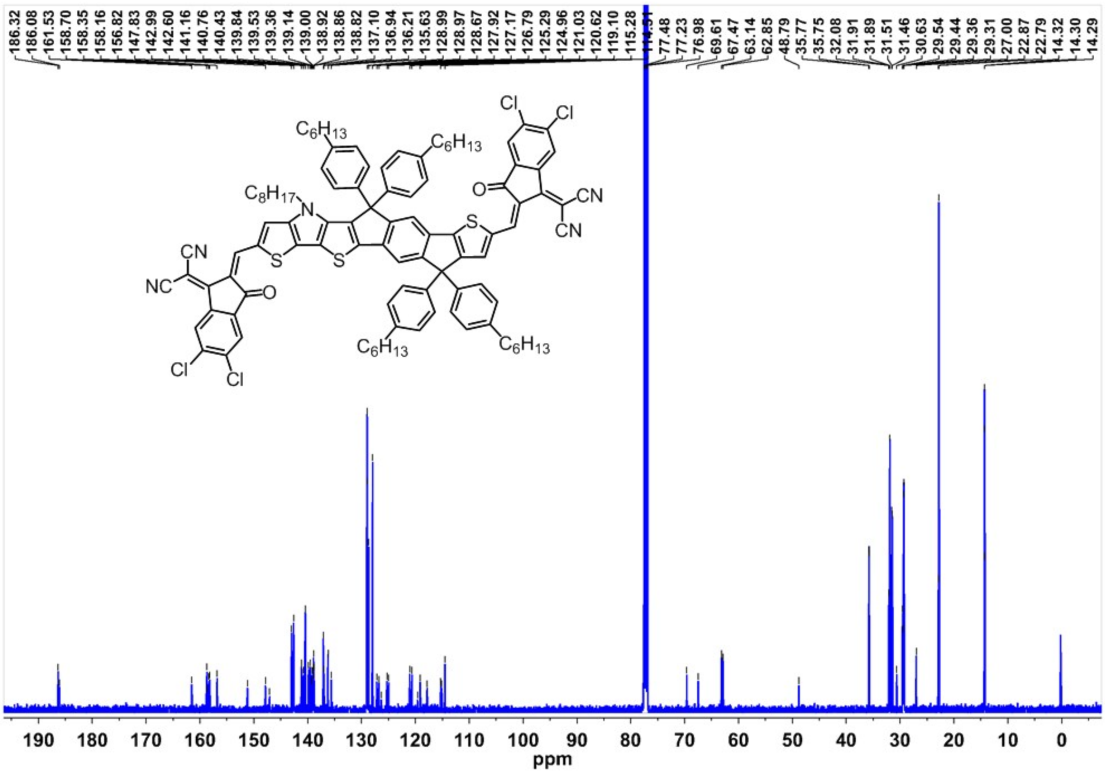

Figure S14. ^{13}C NMR spectrum of IPT-4Cl.

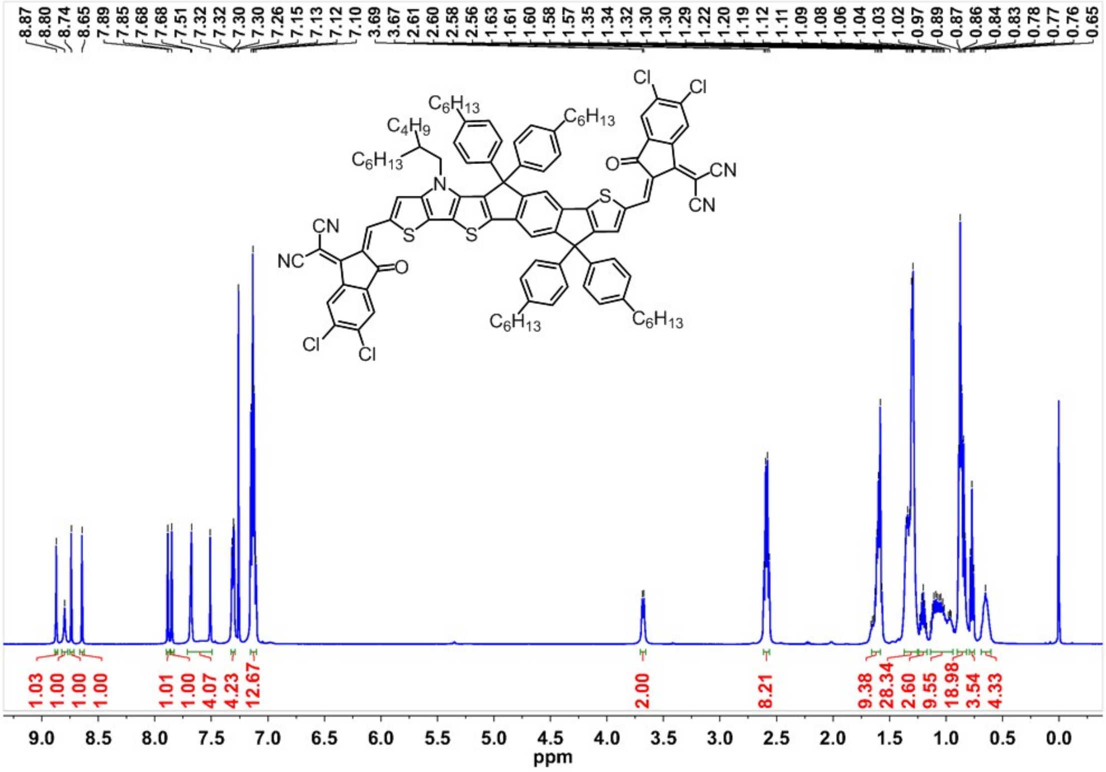

Figure S15. ^{1}H NMR spectrum of IPTBO-4Cl.

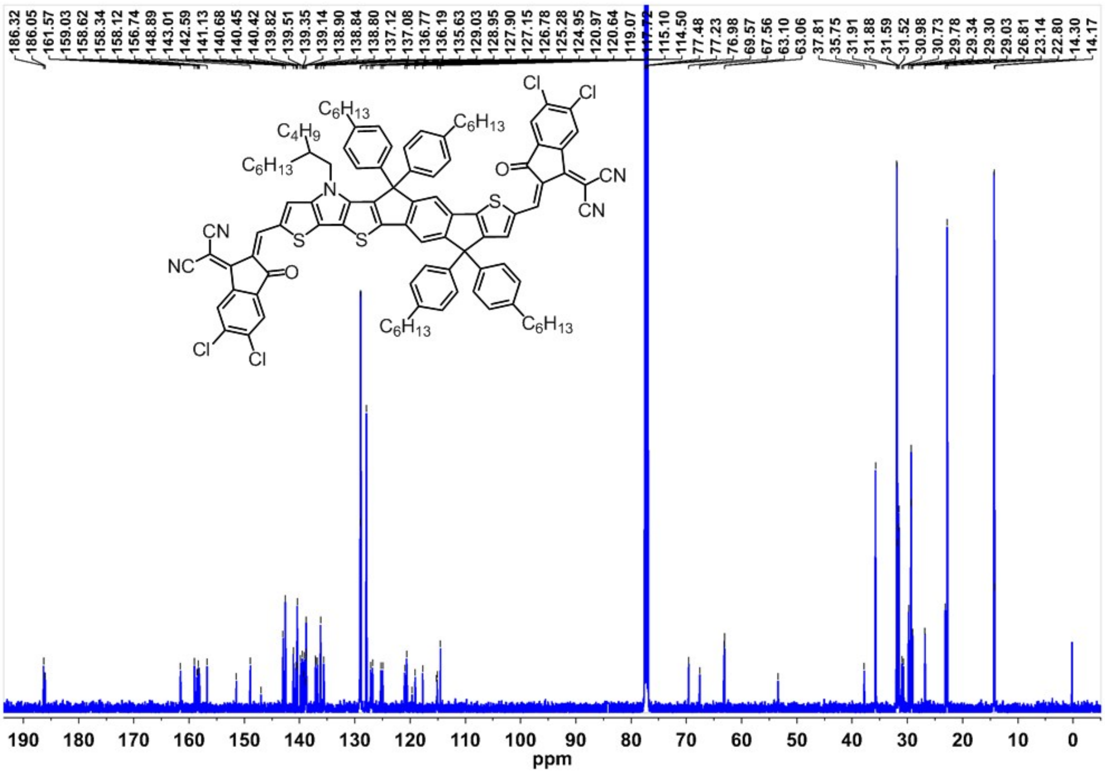

Figure S16. ^{13}C NMR spectrum of IPTBO-4Cl.

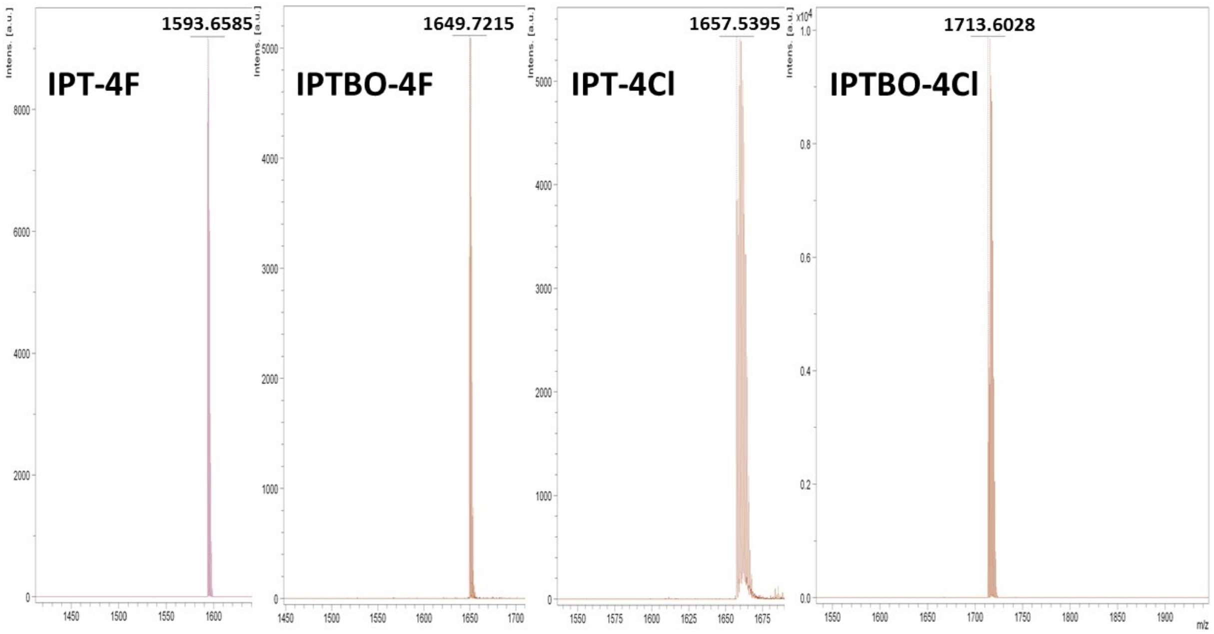

Figure S17. MALDI-TOF MS plots.

2. Methods of Materials Characterization and Theoretical Calculations

^{1}H, ^{13}C, and ^{19}F NMR spectra were obtained on a Bruker AVANCE III 500 MHz instrument with solutions in either $CDCl_3$ or CD_2Cl_2. The matrix-assisted laser desorption/ionization time-of-flight (MALDI-TOF) mass spectra were measured by a Bruker Autoflex TOF/TOF spectrometer. Optical photographs were shot by Panasonic Color CCTV Camera (WV-CP280/G) with objective lens of Nikon CF Plan 100X/0.95 EPI. Similar features of pristine solids could be repeated in different precipitation system, such as dichloromethane/methanol, chloroform/methanol and chlorobenzene/methanol. In detail, 100 mg pristine material was dissolved in good solvent (10 mL), then 40 mL methanol was added dropwise at room temperature and stirring condition. Ultraviolet-visible (UV-Vis) absorption spectra were performed on Thermo Fisher Evolution 220. The thermogravimetric analysis (TGA) was tested on TGA/SDTA851E (Mettler Toledo) with a heating rate of 20°C min^{-1} from 50 to 800°C under nitrogen gas flow. The solubility of acceptors was directly obtained by measuring the dry matter weight of saturated solution. Excess acceptor materials were dissolved in chloroform at ropm temperature. The mixed solution was centrifuged and filtrated to get the saturated solution. Then the dry matter weight in quantified solution was obtained by drying fully. The final solubility can be achieved by a series of calculation and conversion. Differential scanning calorimeter (DSC) analysis was carried out on PerkinElmer Diamond DSC with a heating rate of 40°C min^{-1} from 30 to 280°C in nitrogen atmosphere, and the upper test temperature should be below decomposition point of the acceptors. The DSC tests were conducted with two cycles of heating and cooling. Cyclic voltammetry measurements were carried out on CHI 600D electrochemical workstation. All initial potentials were determined in a 0.1 M Bu_4NPF_6 acetonitrile solution under N_2 atmosphere at a scan rate of 50 mV s^{-1} and corrected against ferrocene/ferrocenium (Fc/Fc^+). A Bruker Multimode 8 atomic force microscopy (AFM) instrument was performed in contact mode to obtain morphology images. TEM tests were performed by FEI TECNAI G2 20 LaB6. Contact angle tests were performed by Kruss DSA100. Grazing-incidence wide-angle X-ray scattering (GIWAXS) was measured at 13A beam line of National Synchrotron Radiation Research Center (NSRRC, Taiwan), and were provided technical support by Ceshigo Research Service, www.ceshigo.com. All samples for GIWAXS were radiated at 12.13 keV X-ray with an incident angle of 0.10~0.15°. The contact angle test and GIWAXS measurement of pristine acceptors used the untreated films.

Theoretical simulation and calculation of molecular comformation, size, area, surface electrostatic potential, and potential energy surface scan were based on density functional theory (DFT) with the B3LYP/6-31G (d, p) basis set. After the molecules were optimized and calculated by DFT, the files of molecular calculation were further used to calculate electrostatic potential by a software of Multiwfn. Molecular surface electrostatic potential was mapped by a software of VMD. Van der Waals surface is defined by electron density level of 0.001 e $Bohr^{-3}$, and all molecular size information was calculated by Multiwfn. Nota that the backbone areas of DTP-T-4F and DTP-T-4Cl were calculated without the four aryl side chains so that we can simplify the calculation and compare the area difference intuitively

3. Device Fabrication and Measurement

The patterned indium tin oxide (ITO) coated glass substrates (sheet resistance 15 Ω sq^{-1}) were consecutively cleaned in ultra-sonic baths containing detergent, de-ionized water, ethanol, respectively. The cleaned ITO substrates were blow-dried by high-purity nitrogen gas and then treated by oxygen plasma for 1 min to improve its work function and clearance. Subsequently, PEDOT:PSS thin films were fabricated on the cleaned ITO substrates by spin-coating methods at 5000 rounds per minute (RPM) for 30 s, and then annealed at 150°C for 10 min under atmospheric conditions. Then ITO substrates coated with PEDOT:PSS films were transferred to a high-purity nitrogen-filled glove box to prepare active layers. The PM6:IPT-4F, PM6:IPTBO-4F, PM6:IPT-4Cl, and PM6:IPTBO-4Cl with 1:1 weight ratio were dissolved in chloroform to prepare 15 mg mL^{-1} binary blend solutions, respectively. N,N'-bis(3-(dimethylamino)propyl)perylene-3,4,9,10-tetracarboxylic diimide (PDIN, purchased from Solarmer Materials Inc.) was dissolved in methanol with addition of 0.25 vol% acetic acid to prepare 2 mg mL^{-1} solution. The prepared binary blend solution were spin-coated on

PEDOT:PSS modified ITO substrates at 2000 RPM for 40s in high-purity nitrogen-filled glove box. The prepared active layers were annealed with CS_2 solvent vapor for 60 s and then annealed at 80°C for 5 min. After that, a PDIN solution was spin-coated onto active layers at 5000 RPM for 30 s. Finally, Al electrode is deposited by thermal evaporation under vacuum of 10^{-5} Pa. The active area of cell is 3.8 mm^2, which is defined by the overlapping area of ITO and Al electrode.

The current-voltage (*J-V*) characteristics of all PSCs were measured in high-purity nitrogen-filled glove box using Keithley 2400 source meter. AM 1.5G irradiation at 100 mW cm^{-2} was provided by An XES-40S2 (SAN-EI Electric Co. Ltd.) solar simulator (AAA grade, 70 × 70 mm^2 photo beam size), which was calibrated by standard silicon solar cells (purchased from Zolix INSTRUMENTS CO, LTD). The external quantum efficiency (EQE) spectra of PSCs were measured in air conditions by a Zolix Solar Cell Scan 100.

4. Data of Material Properties

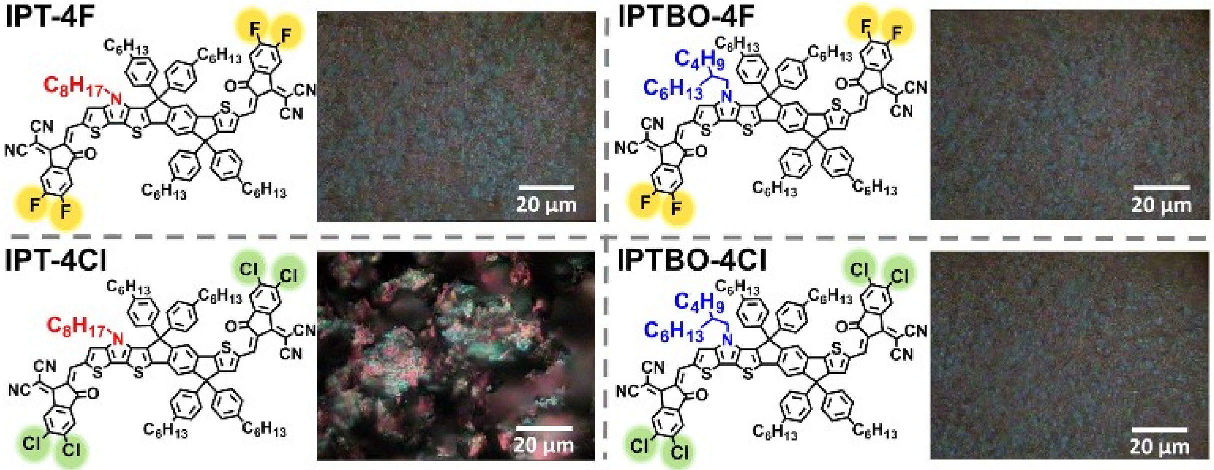

Fig. S18 Molecular structures of the asymmetric FRAs and the corresponding optical photographs of pristine solids precipitated from dichloromethane/methanol solutions.

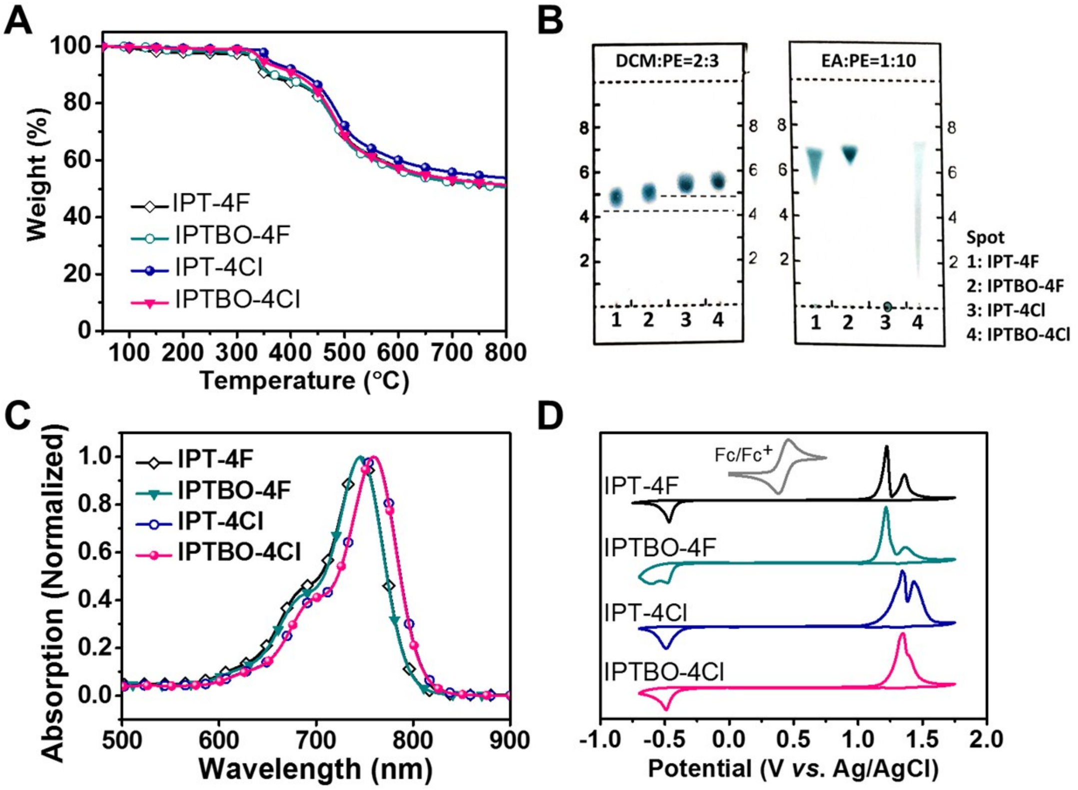

Figure S19. A) Thermogravimetric analysis traces, B) TLC elution profiles, C) Absorption spectra in chloroform solutions, and D) Cyclic voltammetry curves for the FRAs.

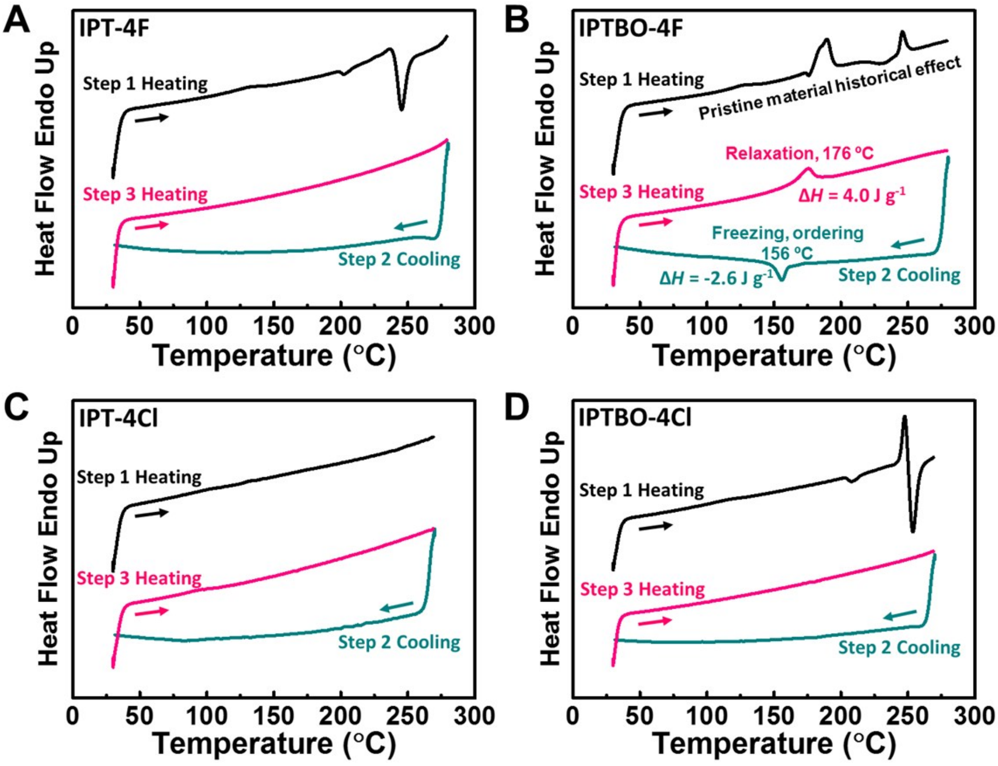

Figure S20. DSC analysis plots.

5. Data of Device Performance

Table S1. Statistic data of binary single-junction OSCs based on asymmestrical FRAs.

Active layer a)	J_{SC} [mA cm^{-2}]	V_{OC} [V]	FF [%]	PCE [%]	Reference
PM6/IPTBO-4Cl	23.2	0.893	72.6	15.0	**This work**
PM6/IPT-4F	22.1	0.914	74.2	15.0	**This work**
PM6/IPTBO-4F	22.1	0.917	72.5	14.7	**This work**
PM6/IPT-4Cl	23.2	0.893	70.4	14.4	**This work**
PBDB-T/IPT-2F	22.4	0.860	72.4	14.0	[2]
PBDB-TF/IT-3F	20.3	0.900	75.5	13.8	[3]
PBDB-T/a-BTTIC	20.3	0.904	74.0	13.6	[4]
PM6/IDT6CN-M	16.6	1.04	77.1	13.3	[5]
PM7/IDT6CN-M	16.4	1.05	77.5	13.3	[5]
J71/ZITI-3F	20.7	0.900	71.5	13.2	[6]
PBT1-C/TTPT-T-2F	18.5	0.915	75.1	12.7	[7]
PBDB-T/MeIC1	18.3	0.927	74.1	12.6	[8]
PBDB-T/IDT8CN-M	17.1	0.920	78.9	12.4	[9]
PM6/IDT6CN-TM	17.4	0.953	74.7	12.4	[10]
PBDB-T/IPTTT-2F	20.0	0.894	69.3	12.3	[2]
PBT1-C/SePTTT-2F	18.0	0.895	75.9	12.2	[11]
PBT1-C/TTPTTT-4F	19.4	0.863	72.1	12.1	[12]
PBDB-T/*a*-IT-2OM	18.1	0.930	71.5	12.1	[13]
PBT1-C/TPTTT-2F	17.6	0.916	74.5	12.0	[14]
PBT1-C-2Cl/IDTT-2F-Th	17.8	0.912	73.9	12.0	[15]

a) Only the statistics with PCE over 12%.

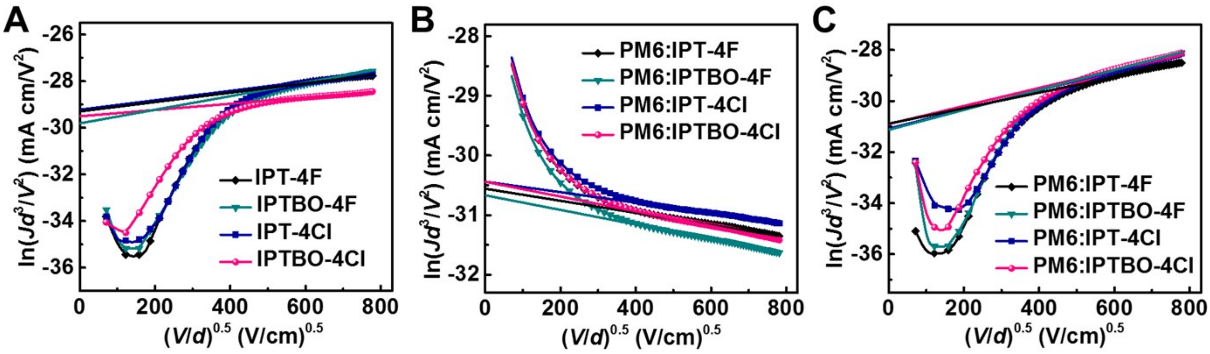

Figure S21. A) Electron mobility plots of the pristine acceptors. B) Hole mobility plots of blend films. C) Electron mobility plots of blend films.

Table S2. Hole and electron mobilities of the blend films

BHJ Layer	μ_h [cm^2 V^{-1} s^{-1}]	μ_e [cm^2 V^{-1} s^{-1}]	μ_h/μ_e
PM6:IPT-4F	1.80×10^{-4}	1.28×10^{-4}	1.41
PM6:IPTBO-4F	1.65×10^{-4}	1.04×10^{-4}	1.59
PM6:IPT-4Cl	1.98×10^{-4}	1.09×10^{-4}	1.82
PM6:IPTBO-4Cl	1.96×10^{-4}	1.24×10^{-4}	1.58

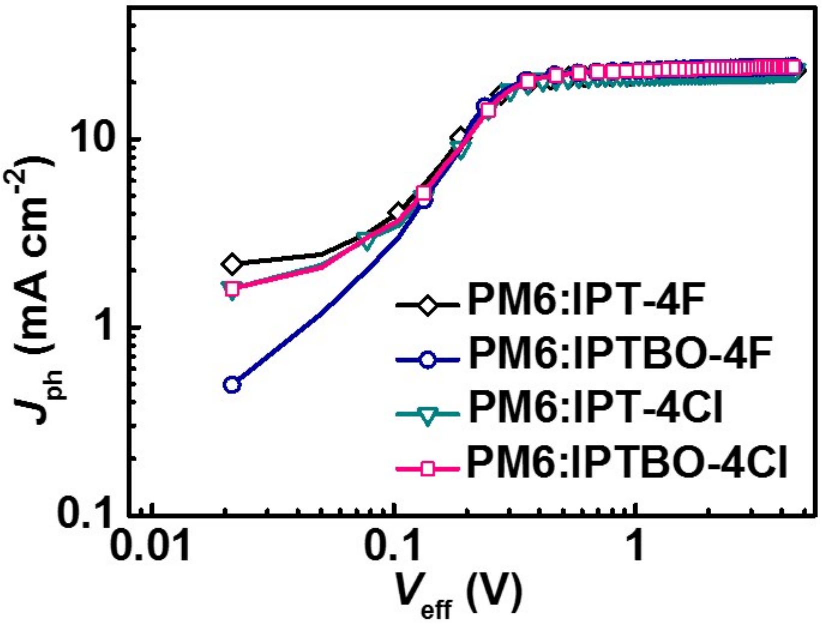

Figure S22. Photocurrent density (J_{ph}) plotted with effective voltage (V_{eff}).

Table S3. Analysis data of J_{ph}-V_{eff} curvers.

BHJ Layer	J_{ph1} [mA cm^{-2}]$^{a)}$	J_{ph2} [mA cm^{-2}]$^{b)}$	J_{sat} [mA cm^{-2}]$^{c)}$	J_{ph1}/J_{sat} [%]	J_{ph2}/J_{sat} [%]
PM6:IPT-4F	22.08	19.57	22.90	96.42	85.46
PM6:IPTBO-4F	22.08	19.49	22.95	96.21	84.92
PM6:IPT-4Cl	23.18	20.34	24.10	96.18	84.40
PM6:IPTBO-4Cl	23.15	20.45	24.05	96.26	85.03

$^{a)}$ J_{ph} values under short-circuit conditions. $^{b)}$ J_{ph} values under maximum output conditions. $^{c)}$ J_{sat} defined as the roughly constant point of the short-circuit current density.

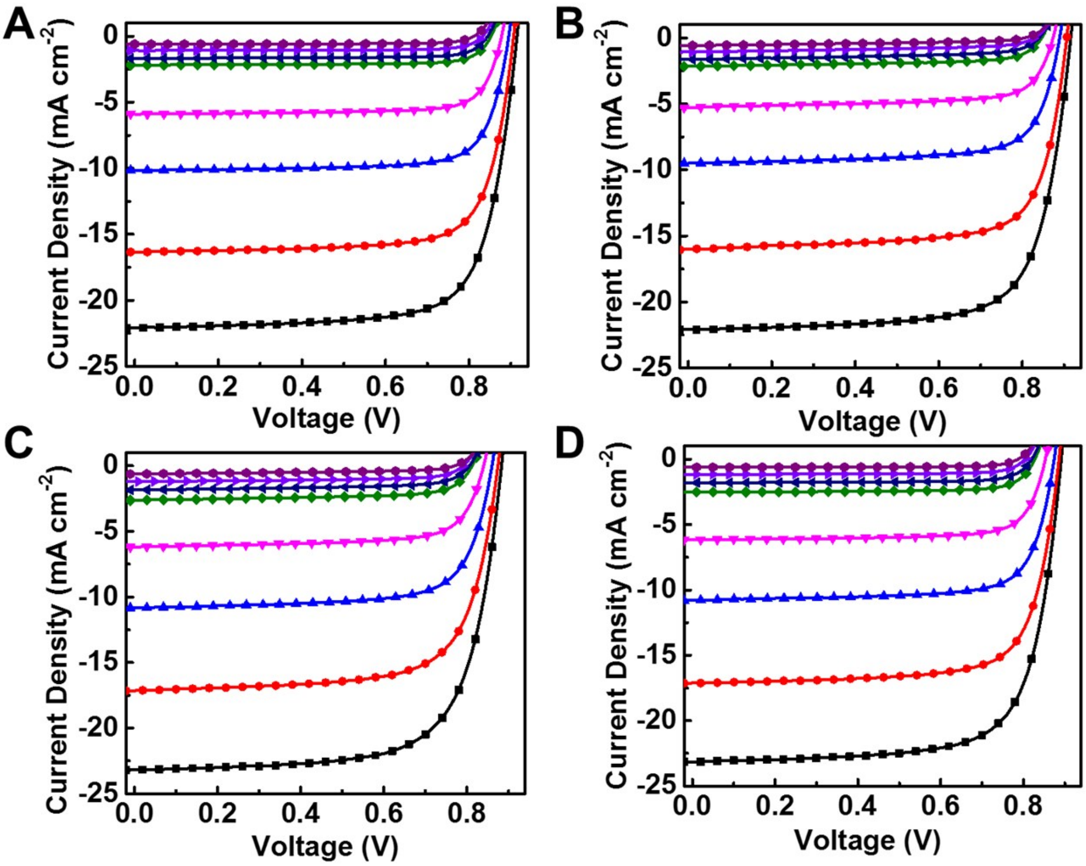

Figure S23. *J*-*V* curves under different light intensities of 2.5, 5, 8, 10, 25, 50, 80, and 100 mW cm^{-2}.

6. Images of AFM and TEM Tests

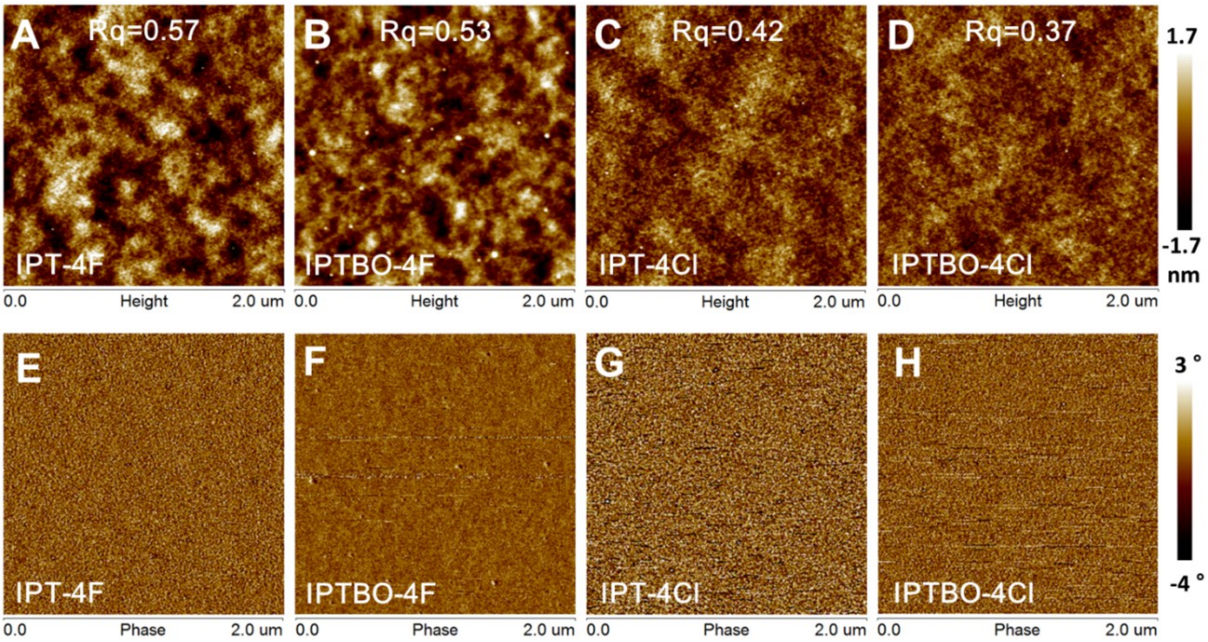

Figure S24. A-D) AFM height images of the pristine acceptor films. E-H) AFM phase images of the pristine acceptor films

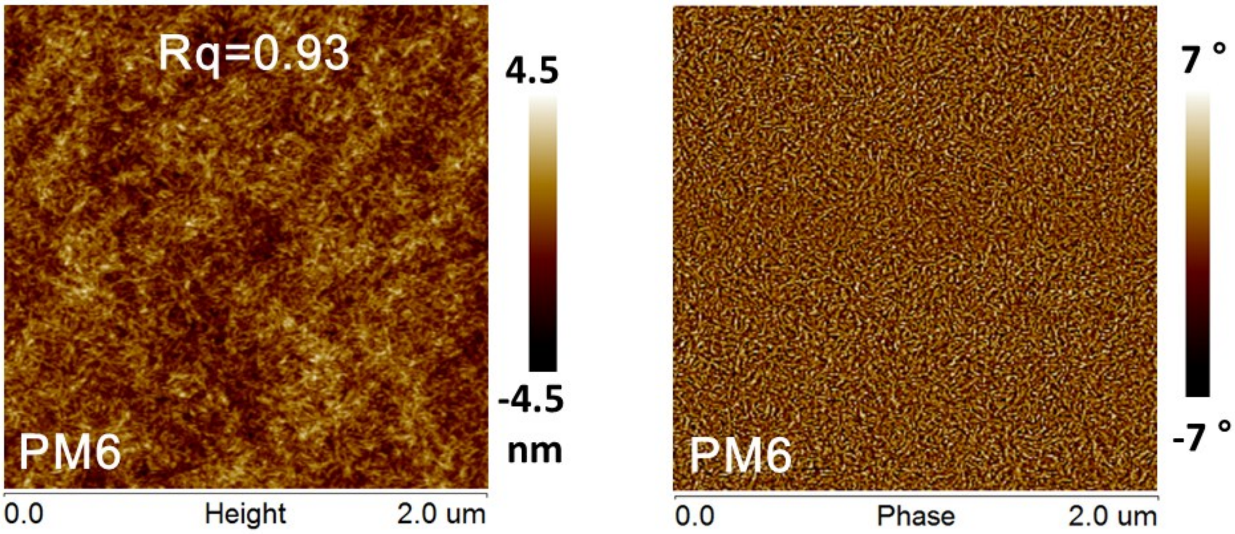

Figure S25. AFM height and phase images of pristine PM6.

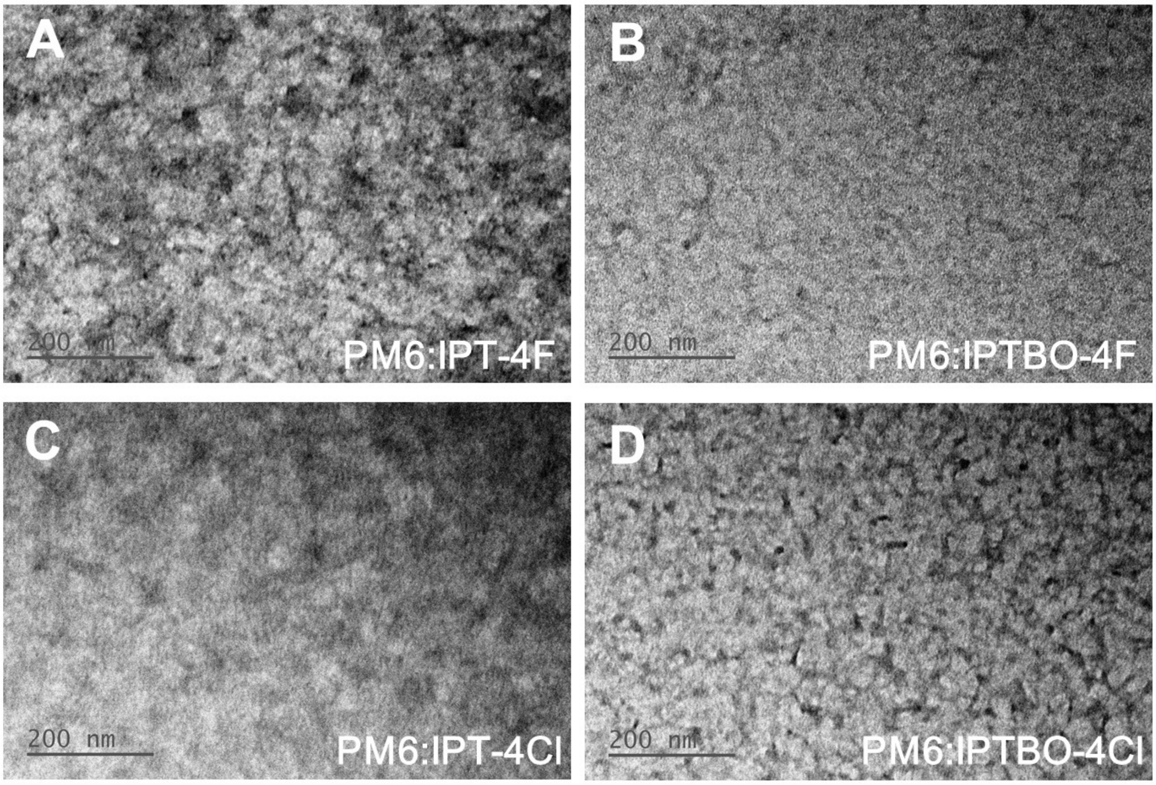

Figure S26. TEM images of the blend films.

References

1 R. Geng, X. Song, H. Feng, J. Yu, M. Zhang, N. Gasparini, Z. Zhang, F. Liu, D. Baran and W. Tang, *ACS Energy Lett.*, 2019, **4**, 763-770.

2 L. Yang, X. Song, J. Yu, H. Wang, Z. Zhang, R. Geng, J. Cao, D. Baran and W. Tang, *J. Mater. Chem. A*, 2019, **7**, 22279-22286.

3 B. Gao, H. Yao, J. Hou, R. Yu, L. Hong, Y. Xu and J. Hou, *J. Mater. Chem. A*, 2018, **6**, 23644-23649.

4 W. Gao, T. Liu, J. Li, Y. Xiao, G. Zhang, Y. Chen, C. Zhong, X. Lu, H. Yan and C. Yang, *J. Mater. Chem. A*, 2019, **7**, 11053-11061.

5 Q. Fan, T. Liu, W. Gao, Y. Xiao, J. Wu, W. Su, X. Guo, X. Lu, C. Yang, H. Yan, M. Zhang and Y. Li, *J. Mater. Chem. A*, 2019, **7**, 15404-15410.

6 J. Zhang, W. Liu, S. Chen, S. Xu, C. Yang and X. Zhu, *J. Mater. Chem. A*, 2018, **6**, 22519-22525.

7 X. Li, C. Li, L. Ye, K. Weng, H. Fu, H. S. Ryu, D. Wei, X. Sun, H. Y. Woo and Y. Sun, *J. Mater. Chem. A*, 2019, **7**, 19348-19354.

8 W. Gao, Q. An, C. Zhong, Z. Luo, R. Ming, M. Zhang, Y. Zou, F. Liu, F. Zhang and C. Yang, *Chem. Sci.*, 2018, **9**, 8142-8149.

9 W. Gao, T. Liu, C. Zhong, G. Zhang, Y. Zhang, R. Ming, L. Zhang, J. Xin, K. Wu, Y. Guo, W. Ma, H. Yan, Y. Liu and C. Yang, *ACS Energy Lett.*, 2018, **3**, 1760-1768.

10 W. Gao, F. Wu, T. Liu, G. Zhang, Z. Chen, C. Zhong, L. Zhu, F. Liu, H. Yan and C. Yang, *J. Mater. Chem. A*, 2019, **7**, 2412-2420.

11 C. Li, T. Xia, J. Song, H. Fu, H. S. Ryu, K. Weng, L. Ye, H. Y. Woo and Y. Sun, *J. Mater. Chem. A*, 2019, **7**, 1435-1441.

12 C. Li, J. Song, L. Ye, C. Koh, K. Weng, H. Fu, Y. Cai, Y. Xie, D. Wei, H. Y. Woo and Y. Sun, *Sol. RRL*, 2019, **3**, 1800246.

13 M. Li, Y. Zhou, J. Zhang, J. Song and Z. Bo, *J. Mater. Chem. A*, 2019, **7**, 8889-8896.

14 J. Song, C. Li, L. Ye, C. Koh, Y. Cai, D. Wei, H. Y. Woo and Y. Sun, *J. Mater. Chem. A*, 2018, **6**, 18847-18852.

15 L. Ye, Y. Xie, Y. Xiao, J. Song, C. Li, H. Fu, K. Weng, X. Lu, S. Tan and Y. Sun, *J. Mater. Chem. A*, 2019, **7**, 8055-8060.